JOURNAL OF THERMOPHYSICS AND HEAT TRANSFER
Vol. 23, No. 1, January–March 2009

Technical Notes

TECHNICAL NOTES are short manuscripts describing new developments or important results of a preliminary nature. These Notes should not exceed 2500 words (where a figure or table counts as 200 words). Following informal review by the Editors, they may be published within a few months of the date of receipt. Style requirements are the same as for regular contributions (see inside back cover).

New Asymptotic Temperature–Heat Flux Integral Relationship in Cylindrical Coordinates

J. I. Frankel*
University of Tennessee, Knoxville, Tennessee 37996-2210

DOI: 10.2514/1.36825

Nomenclature

a	=	nozzle throat radius, m
b	=	spread factor for Gauss function, s
C	=	heat capacity, kJ/(kg°C)
$f(t)$	=	firstkind boundary condition, °C
f_c	=	filter cutoff frequency, $n_c/t_{\max}$, Hz
f_j	=	discrete sensor temperature at time t_j, °C
G	=	Green's function, m^{-2}
$\tilde{G}$	=	asymptotic Green's function, m^{-2}
$I_0(v)$	=	modified Bessel function of the first kind of order zero
k	=	thermal conductivity, W/(m°C)
L_0	=	adjoint differential operator
M	=	maximum number of data points
n_c	=	cutoff value of data in defining cutoff frequency
p_i	=	random number drawn from the interval [−1, 1]
q''	=	heat flux, W/m^2
q''_0	=	peak heat flux value in boundary condition, W/m^2
$\tilde{q}''$	=	asymptotic heat flux, W/m^2
R	=	arbitrary location, m
r	=	radial variable, m
r_m	=	sensor location, $m = 1, 2$, m
r_0	=	radial variable, m
s	=	dummy time variable, s
T	=	temperature, °C
$T_f(r_m, t)$	=	filtered data, °C
$T_{m,j}$	=	discrete noisy temperature, °C
T_0	=	initial temperature, °C
$\tilde{T}$	=	asymptotic temperature, °C
t	=	time, s
$t_{\max}$	=	maximum time in experiment, s
t_0	=	dummy time variable, s
u	=	dummy time variable, s
v	=	dummy argument for Bessel function
W	=	outside diameter of nozzle casing, m
w_r	=	weight function
x	=	spatial variable, m
α	=	thermal diffusivity $[k/(\rho C)]$, m^2/s
γ_j	=	noise, °C
Δt	=	time between samples, $t_{\max}/M$, s
δ	=	Dirac delta function
ϵ	=	small time increment, s
η	=	arbitrary position, m
ρ	=	density, kg/m^3
σ	=	time factor where Gauss function peaks, s
ω_c	=	cutoff (circular) frequency, $2\pi f_c$, rad/s
ω_m	=	noise factor at spatial sites

Subscripts

i, j	=	index for discrete time, $i = 1, 2, \ldots, M$
m	=	probe spatial locations, $m = 1, 2$

Introduction

CHANNEL flows play a key role in many aerospace applications. This paper studies a nozzle geometry which has either one or two internally mounted thermocouples located at different radial positions at the throat region. A linear, transient, one-dimensional, axisymmetric, radially infinite ($r > a =$ throat radius) heat conduction model is proposed in the vicinity of the nozzle-throat region for specifically estimating the heat flux corresponding to embedded temperature sensor sites. Without loss of generality, it is assumed that a trivial initial condition exists. The experimental run times are sufficiently short such that the nozzle's casing remains at the initial condition and hence justifying the infinite radial model. In practice, this time span could extend several minutes, depending on the nozzle thermophysical properties and dimensions. The initial goal of this study is to explicitly indicate that the heating/cooling rate $\partial T/\partial t$ plays a significant role in governing stability [1–7] in the prediction of the local heat flux. Frankel et al. [1–7] have developed a novel mathematical, theoretic formalism applicable to higher dimensional half-space (Cartesian) analyses based on both Green's functions and Fourier transforms. The key manipulation involves developing a regularized integral equation for the temperature. Singular geometries often introduce analytic difficulties due to the complications associated with special functions and their integral relations. However, this paper analytically demonstrates the importance of the heating/cooling rate for early-time solutions. The user must stabilize or regularize the temperature data with respect to the time derivative to arrive at good heat flux predictions. Hence, proper digital filtering [3,6] or the direct measurement of the heating rate [8] is required.

The key fundamental analytic result of this paper indicates that, for early times (which depends on the thermal diffusivity), the heat flux $q''(r, t)$ strongly depends on both the temperature T and heating rate $\partial T/\partial t$ (°C/s) as

$$\tilde{q}''(r,t) \sim \frac{k\tilde{T}(r,t)}{2r} + \sqrt{\frac{\rho Ck}{\pi}} \int_{t_0=0}^{t} \frac{\partial \tilde{T}}{\partial t_0}(r,t_0) \frac{\mathrm{d}t_0}{\sqrt{t-t_0}} \qquad r \geq a, \quad \frac{r^2}{2\alpha t} \to \infty \tag{1}$$

where the $\sim$ symbol is a reminder to the reader that it is an early-time

Presented as Paper 1189 at the 46th AIAA Aerospace Meeting and Exhibit, Reno, NV, 7–10 January 2008; received 24 January 2008; revision received 17 July 2008; accepted for publication 21 July 2008.

*Professor, Mechanical, Aerospace and Biomedical Engineering Department, Corresponding Author; vfrankel@earthlink.net. Associate Fellow AIAA.

solution and a trivial initial condition $T(r,0) = 0°C$ is assumed. The reader also is reminded that in asymptotics, the value of ∞ is often not large since $r^2/(2\alpha t) \gg 1$. Equation (1) is developed under the assumption of constant thermophysical properties. Hence, all hope for resolving the local heat flux (for all time) implicitly relies on a good representation of the heating rate in arriving at an accurate heat flux prediction. The inversion, via Abel regularization [6], of Eq. (1) leads to

$$\tilde{T}(r,t) \sim \frac{1}{\sqrt{\rho C k \pi}} \int_{u=0}^{t} \left(\tilde{q}''(r,u) - \frac{k}{2r} \tilde{T}(r,u) \right) \frac{\mathrm{d}u}{\sqrt{t-u}} \qquad r \geq a \qquad \frac{r^2}{2\alpha t} \to \infty \tag{2}$$

Kulish et al. [9,10] studied the half-space planar geometry involving the inverse relationship analogous to Eq. (2) by the Laplace transform method. In these investigations [9,10], the input involved heat flux and it was desired to obtain the resulting temperature. From viewing Eq. (2), the determination of the heat flux requires the resolution of a first-kind Volterra equation with known temperature data. First-kind equations are known to be mildly ill-posed [11–13]. Equations (1) and (2) are equivalent and thus suffer the same ill-posed fate. Thus, using Eq. (2) does not change or alter or assist in resolving the heat flux based on temperature measurements. A mathematical proof to the problem is provided in [3] and clearly indicates the culprit (i.e., $\partial T/\partial t$).

Nozzle Throat Heat Conduction Model in Cylindrical Coordinates

The physical application of interest is schematically displayed in Fig. 1. This figure indicates high-speed flow through a nozzle that can be composed of conventional materials such as copper, stainless steel, etc., or more exotic materials, though isotropic/bulk properties are assumed. A typical set of geometric parameters could involve a throat diameter of 5 cm and exit plane diameter of 10 cm. The length of the nozzle region could extend 25 cm. These geometric values are representative and provide a physical sense of size. Here, the exit plane to throat diameter ratio is merely 2. A typical Mach number at the exit plane could be 2. If a combustor is located upstream, then high-temperature gases are flowing through the nozzle for expansion. If run times are relatively short, then the region

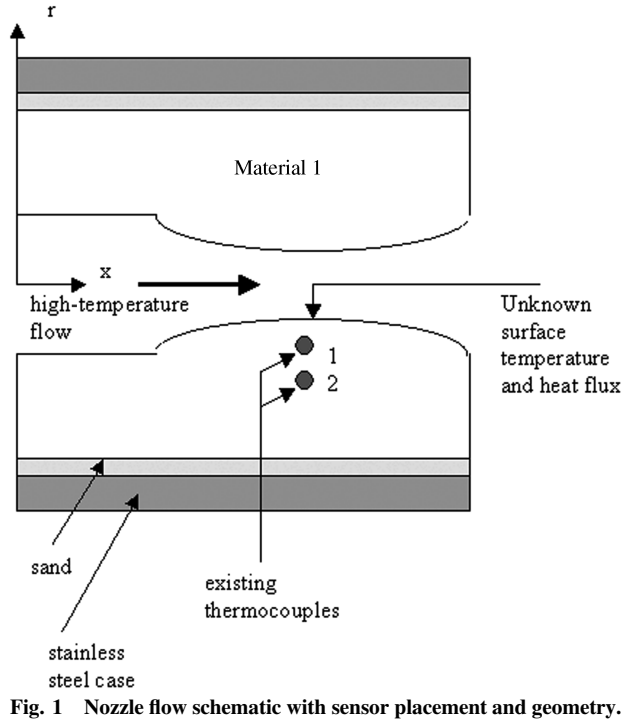

Fig. 1 Nozzle flow schematic with sensor placement and geometry.

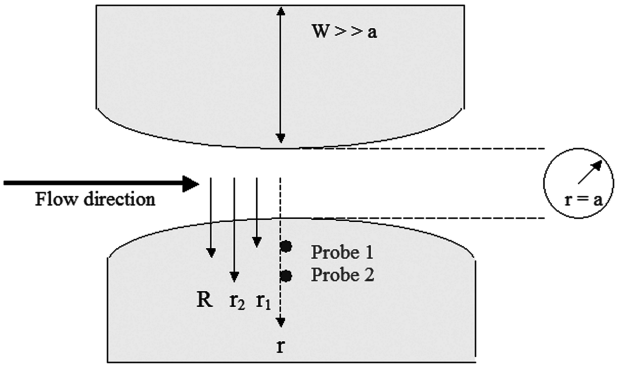

Fig. 2 Simplified model for developing cylindrical analysis.

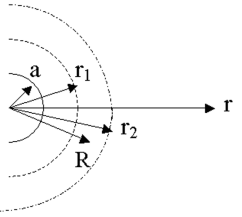

Fig. 3 Coordinate system for cylindrical analysis.

interfacing the sand region remains at the initial temperature. Thus, in the time span of interest, the radial region can be modeled to extend to infinity and hence permits mathematical simplification. Figure 2 portrays the region associated with the idealized nozzle region, whereas Fig. 3 provides the coordinate system for this investigation. For the moment, our particular interest merely lies in predicting the heat flux at the sensor site based on temperature measurements. Hence, owing to the relative flatness near the throat region, as indicated in Fig. 2, we adopt a hollow-cylinder model as a first attempt for estimating the heat flux at a corresponding temperature sensor location. Practically speaking, only a limited number of temperature sensors can be installed in many applications.

The surface prediction for temperature and heat flux using one or more embedded sensors actually involves two inverse problems. The focus of this Note involves the first inverse problem located at the sensor site in the semi-infinite region $r > a$. The first inverse problem involves determining the local heat flux at the sensor site based on the time history of temperature. The second inverse problem would involve the projection from the sensor site(s) to the surface. The objective of this Note involves deriving a short-time integral relationship between heat flux and temperature (or heating/cooling rate) based on a unified theoretic approach presently under development [4–7]. This section provides 1) the simplified model and 2) the basic early-time results referring the reader to the Appendix for the early-time derivation.

Simplified Model

The constant property, one-dimensional, transient heat equation in cylindrical coordinates is given by [14]

$$\frac{\partial T}{\partial t}(r,t) = \frac{\alpha}{r}\frac{\partial}{\partial r}\left(r \frac{\partial T}{\partial r}(r,t) \right), \qquad r \in [R,\infty), \qquad t \geq 0 \tag{3a}$$

subject to the boundary conditions

$$T(R,t) = f(t) \tag{3b}$$

$$T(\infty,t) = T_0, \qquad t \geq 0 \tag{3c}$$

and initial condition

$$T(r,0) = T_0, \qquad r \in [R,\infty) \tag{3d}$$

where $r = R$ could represent the physical geometry $r = R = a$ or a sensor location $r = R = r_m$, $m = 1, 2$. At a sensor location, only discrete values are possible and hence, Eq. (3b) should be expressed as

$$T(r_m, t_j) = f_j, \qquad j = 1, 2, \ldots, t_j = j\Delta t, \qquad m = 1, 2 \quad (3e)$$

where $f_j = f(t_j) + \gamma_j$ with $f(t_j)$ representing the exact, uncontaminated data, whereas γ_j, $j = 1, \ldots, M$ are the local errors for the total data set containing M samples. Without loss of generality, we let $T_0 = 0°\text{C}$.

Solution Methodology

It is imperative to analytically demonstrate that the heating rate $\partial T/\partial t$ strongly influences the prediction of heat flux in nonplanar geometries at an arbitrary radial position. To date, this has not been demonstrated. The analytic complexities associated with special functions often preclude detailed analytic interrogation for the entire time domain. However, we demonstrate that an early-time analysis brings out the necessary details, confirming the importance of the heating rate in singular geometries. This section provides a summary of results, whereas the Appendix contains the detailed integral relationship derivation.

The early-time integral relationship is derived with the aid of the boundary element method [15] (BEM), which tends to use the infinite domain Green's function, and a singular integral equation regularization concept involving iterated kernels. The two-dimensional study presented in [4] clearly demonstrates the methodology for identifying the proper integral operator for regularization based on a novel observation involving the construction of the Green's function. To begin, we develop the general expression for the temperature in terms of the boundary conditions. This provides us with the starting point to make several key observations. The BEM involves operating on Eq. (3a), after replacing the independent variables by (r_0, t_0), with the Green's function, denoted by $G(r, t/r_0, t_0)$, and integrating over the volume element and all time to obtain

$$\lim_{\epsilon\to 0}\int_{t_0=0}^{t+\epsilon}\int_{r_0=a}^{\infty} L_o[T(r_0,t_0)]G(r,t/r_0,t_0)2\pi r_0\,\mathrm{d}r_0\,\mathrm{d}t_0 = 0 \qquad r \geq a, \qquad t \geq 0 \quad (4a)$$

where the Green's function is expressed in the $G(\text{effect}/\text{cause})$ form [16]. The operator L_0 is given by

$$L_0 = \frac{\partial}{\partial t_0} - \frac{\alpha}{r_0}\frac{\partial}{\partial r_0}\left(r_0\frac{\partial}{\partial r_0}\right) \quad (4b)$$

where ϵ is introduced to invoke the causality principle. For the present investigation, we define the Green's function based on the full-space ($r \geq 0$) system, namely,

$$\frac{\partial G}{\partial t_0} + \frac{\alpha}{r_0}\frac{\partial}{\partial r_0}\left(r_0\frac{\partial G}{\partial r_0}\right) = -\frac{\delta(r_0 - r)\delta(t_0 - t)}{r_0} \qquad r \in (0, \infty), \qquad t \geq t_0 \quad (4c)$$

The resulting Green's function is [17]

$$G(r, t/r_0, t_o) = \frac{1}{4\pi\alpha(t - t_0)}e^{-\frac{r^2+r_0^2}{4\alpha(t-t_0)}}I_0\left(\frac{rr_0}{2\alpha(t - t_0)}\right) \qquad (r, r_0) \geq 0, \qquad t \geq t_0 \quad (4d)$$

where $I_0(v)$ is the modified Bessel function of the first kind of order zero with argument v. Upon invoking compact support at infinity, the resulting solution for the temperature distribution becomes

$$w_r T(r,t) = a\alpha\int_{t_0=0}^{t}\left[G(r,t/a,t_0)\frac{q''(a,t_0)}{k} + T(a,t_0)\frac{\partial G}{\partial r_0}(r,t/a,t_0)\right]\mathrm{d}t_0, \qquad r \geq a, \qquad t \geq 0 \quad (5a)$$

where the Green's function $G(r, t/r_0, t_0)$ is given in Eq. (4d). At this junction, no assumptions are invoked at the boundary $r = a$. The weight function conforms with the boundary element method [16] and is set to unity for $r > a$. Using Fourier's law $q''(r,t) = -k(\partial T/\partial r)(r,t)$, we can obtain the corresponding heat flux, $q''(r,t)$ as

$$w_r q''(r,t) = -k\frac{\partial T}{\partial r}(r,t) = -ka\alpha\int_{t_0=0}^{t}\left[\frac{\partial G}{\partial r}(r,t/a,t_0)\frac{q''(a,t_0)}{k} + T(a,t_0)\frac{\partial^2 G}{\partial r\partial r_0}(r,t/a,t_0)\right]\mathrm{d}t_0, \qquad r \geq a, \qquad t \geq 0 \quad (5b)$$

It appears difficult to develop an explicit relationship involving $q''(r,t)$, $T(r,t)$, and $\partial T/\partial t(r,t)$ at arbitrary location $r > a$ for all time $t > 0$, due to the analytic complexities inherent with $G(r, t/r_0, t_0)$, as displayed in Eq. (4d). However, it does appear possible to develop an early-time integral relationship that explicitly demonstrates the importance of the heating rate based on an asymptotic Green's function $\tilde{G}(r, t/r_0, t_0)$ [18], namely,

$$G(r, t/r_0, t_0) \sim \tilde{G}(r, t/r_0, t_0) = \frac{1}{2\pi\sqrt{rr_0}}\left(\frac{e^{-\frac{(r-r_0)^2}{4\alpha(t-t_0)}}}{\sqrt{4\pi\alpha(t - t_0)}}\right), \qquad \frac{rr_0}{2\alpha(t - t_0)} \to \infty \quad (5c)$$

The term in the parentheses can be viewed as the full-space Green's function associated with one-dimensional heat conduction in Cartesian coordinates. This provides the clue on how to obtain the integral relationship, because the remaining portion [coefficient to the Cartesian Green's function shown in Eq. (5c)] depends on space and not time. It can be demonstrated (see the Appendix) that the heat flux at arbitrary $r > a$ for early times ($r^2/2\alpha t \to \infty$) is

$$\tilde{q}''(r,t) \sim \frac{k\tilde{T}(r,t)}{2r} + \sqrt{\frac{\rho Ck}{\pi}}\int_{t_0=0}^{t}\frac{\partial\tilde{T}}{\partial t_0}(r,t_0)\frac{\mathrm{d}t_o}{\sqrt{t - t_0}}, \quad \text{as} \quad \frac{r^2}{2\alpha t} \to \infty \quad (6)$$

$r \geq a$ where $\tilde{T}$, $\tilde{q}''$, and $\partial\tilde{T}/\partial t$ represent early-time approximations for temperature, heat flux, and heating rate, respectively. This expression is similar to the half-space planar solution [6] but with the extra term or geometric correction $k\tilde{T}(r,t)/(2r)$. Equation (6) is a new, fundamental, and practical result demonstrating that the heating rate, $\partial T/\partial t(r,t)$ must be accurately represented when reconstructing the heat flux, $q''(r,t)$ for all $t \geq 0$. It is interesting to note that Eq. (6) reduces to the strictly interfacial (i.e., boundary) condition derived by Buttsworth and Jones [19] using the Laplace transform technique. Unlike [19], the derivation displayed in the Appendix is valid for $r \geq a$.

Digital Filtering

A Gauss filter function for temperature has been devised based on Fourier convolution principles [3,6]. The advantage of such a filter lies in its behavior in both the time and frequency domains. The Fourier transform of a Gauss function produces another Gauss function (i.e., self-reciprocal). Thus, in both time and frequency, the functions are wiggle free. This low-pass filter offers good differentiability properties. The finite number of samples in the original data set now become continuous and could provide additional flexibility when incorporated into numerical schemes, because one is not restricted to using the exact sample times. Hence, the chosen filter is given by

$$T_f(r_m,t)=\frac{\sum_{j=1}^{M} T(r_m,t_j)e^{-\frac{(t-t_j)^2\omega_c^2}{4}}}{\sum_{j=1}^{M} e^{-\frac{(t-t_j)^2\omega_c^2}{4}}}, \qquad m=1,2, \qquad t>0 \tag{7}$$

where $\omega_c = 2\pi f_c$ and equidistant sampling is assumed. Here, f_c is the user-supplied cutoff frequency, which can be estimated from the discrete Fourier transform (DFT) using Wiener filtering concepts [6].

For this study, we now define the numerical procedure for arriving at the heat flux $q''(r_m,t)$ corresponding to the temperature sensor location $r=r_m, m=1,2$. In a nutshell, the process is as follows [6]:

1) Obtain noisy, temperature data $T(r_m,t_j)=T_{m,j}$, $m=1,\ 2$, $j=1,\ldots,M$ from embedded site(s).
2) Interrogate power spectrum at each site to approximate cutoff frequency $f_{c,m}$, $m=1,2$ for Gauss filter.
3) Filter noisy temperature data in accordance to Eq. (7) to obtain $T_f(r_m,t_j)$, $m=1,2$, $j=1,\ldots,M$.
4) Approximate heating/cooling rate $\partial T_f/\partial t(r_m,t)$, $m=1,\ 2$ using filtered data via simple finite differences, though one could analytically obtain this through the filter.
5) Numerically obtain the embedded heat flux $q''(r_m,t)$, $m=1,2$ using Eq. (6).

Results

In this section, we present exact and approximate heat flux results developed using Eq. (1) or Eq. (6) at sensor sites. For the sake of benchmarking, we propose a forward problem based on solving the Gauss heat flux boundary condition

$$q''(a,t)=q_0''e^{-\left(\frac{t-b}{\sigma}\right)^2}, \qquad t\geq 0 \tag{8}$$

where b and σ are geometrically self-explanatory. The resulting surface temperature ($r=a$) and probe site temperatures ($r=r_1, r_2$) are numerically obtained using an analytic solution requiring numerical integration. This is a classical solution and can be found in [14].

Before obtaining the local heat flux, we begin by comparing the Green's function $G(r,t/r_0,t_0)$ given in Eq. (4d) to the asymptotic Green's function $\tilde{G}(r,t/r_0,t_0)$ given in Eq. (5c) for two thermophysically diverse materials (copper and stainless steel). Note that the time variables appear as a difference. For a fixed parameter set $\{\alpha, r_0, r, t-t_0\}$, we can visually view when the early-time assumption breaks down [18]. A detailed study on the breakdown can be found in [18]. All numerical simulations were performed using Mathematica 3.0. Figures 4 and 5 present a comparison between the two Green's functions for copper ($\alpha=1.15$ cm^2/s) and stainless steel ($\alpha=0.042$ cm^2/s), respectively, over the time difference $u=t-t_0$. Here, $r_0=2$ cm and $r=2.25$, 2.5, and 2.75 cm. The solid line represents $G(r,t/r_0,t_0)$, whereas the dashed line represents $\tilde{G}(r,t/r_0,t_0)$. It is interesting to note that the Green's function contains the exact parameters associated with penetration depth and thus permits additional

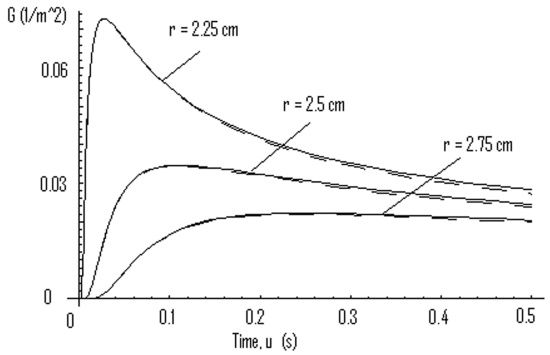

Fig. 4 Comparison between Green's functions (exact, solid line; asymptotic, dashed line) when $r_0=2$ cm for copper ($\alpha=1.15$ cm^2/s) at the indicated r locations.

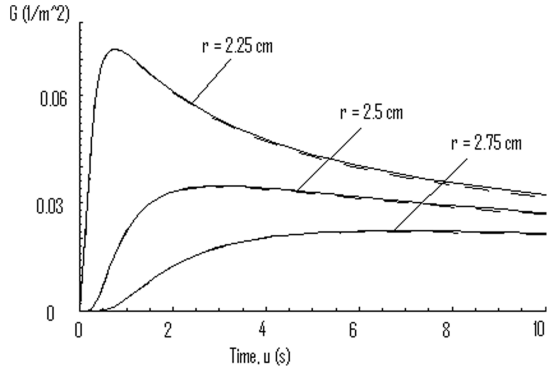

Fig. 5 Comparison between Green's functions (exact, solid line; asymptotic, dashed line) when $r_0=2$ cm for stainless steel ($\alpha=0.042$ cm^2/s) at the indicated r locations.

interpretations. It is evident for the time spans indicated that both Green's functions are nearly identical. For small α, additional time is available for using the asymptotic Green's function $\tilde{G}(r,t/r_0,t_0)$.

Let contaminated data be generated in accordance to

$$T_{m,i}=T(r_m,t_i)+\omega_m\|T(r_m,t)\|_\infty p_i \qquad m=1,2, \qquad i=1,2,\ldots,M \tag{9}$$

where $T(r_m,t)$ is the exact solution at location $r=r_m$, $m=1,2$ and time t, ω_m is the noise factor at each site

$$\|T(r_m,t)\|_\infty=\max_{t\in(0,t_{\max})}|T(r_m,t)|$$

and p_i is the ith random number drawn from the closed interval $[-1, 1]$ based on a uniform probability density function (white noise) with a variance of approximately one-third. For Figs. 6–9, let material 1 shown in Fig. 1 have the following thermophysical and geometrical properties: $\alpha=0.1$ cm^2/s, $k=50$ W/(m°C), $a=2$ cm, $r_1=2.3175$ cm, $r_2=2.635$ cm, and let $M=100$, $q_0''=10$ MW/m^2, $\sigma=0.5$ s, $b=t_{\max}/2$ s, and $t_{\max}=5$ s. Before investigating contaminated data, let us see how the proposed digital filter affects the exact $\omega_m=0$, $m=1,2$ data. Figure 6 presents numerical results for the analytic solution (solid line) and discrete (solid circles) temperature data at $r=a, r_1, r_2$. The filtered data are represented by dashed lines where $f_c=n_c/t_{\max}$, $n_c=15$, as estimated from the DFT [6]. It should be noted that choosing $n_c=20$ does not substantially change the results. It is difficult to distinguish any difference among the analytic (solid line), exact discrete (solid circles), and filtered (dashed line) representations for the temperature data at the two sites r_1 and r_2. Figure 7 contains the corresponding heat fluxes $q''(r,t)$ at the three locations $r=a, r_1, r_2$. The proposed digital filter uses the complete set of data and hence incorporates both future and past times in creating the local, filtered value. Figure 7

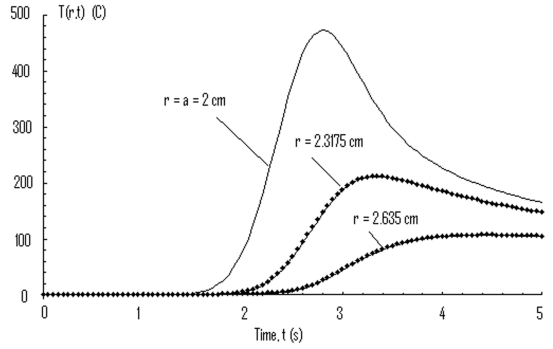

Fig. 6 Exact temperature (solid line), discrete exact data (solid circles), and filtered data (dashed lines) over time when $r=r_1=2.3175$ cm and $r_2=2.635$ cm where $a=2$ cm for material having $k=50$ W/(m°C), $\alpha=0.1$ cm^2/s, and with $M=100$, $n_c=15$, $\omega_m=0$, $m=1,2$ using the imposed Gauss boundary condition, Eq. (8).

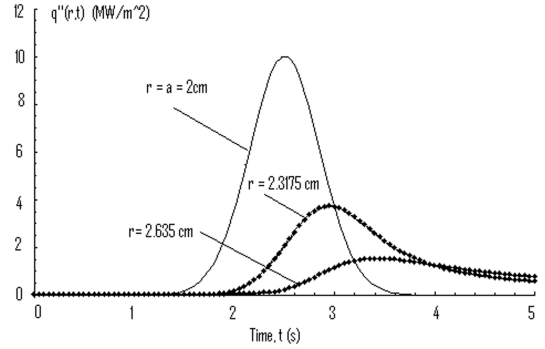

Fig. 7 Heat flux results using noisy temperature data displayed in Fig. 6 at $r = r_1 = 2.3175$ cm, $r = r_2 = 2.635$ cm over time, t: exact (solid line), discrete noisy [solid circles, based on Eq. (1)], and filtered [dashed lines, based on Eq. (1)] for material having $\alpha = 0.1$ cm^2/s, $k = 50$ W/(m°C), and imposed Gauss heat flux boundary condition, Eq. (8), using $M = 100$ data points.

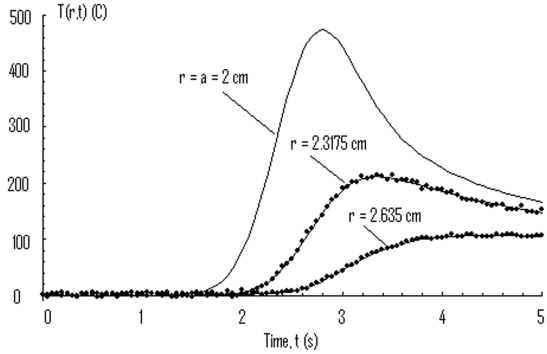

Fig. 8 Noisy ($\omega_m = 0.025$, $m = 1$, 2) temperature data at $r = r_1 = 2.3175$ cm, $r = r_2 = 2.635$ cm over time, t: exact (solid line), discrete noisy [solid circles, Eq. (9)], and filtered [dashed lines, Eq. (7)] for material having $\alpha = 0.1$ cm^2/s, $k = 50$ W/(m°C), and surface temperature ($r = a = 2$ cm) resulting from imposed Gauss heat flux condition, Eq. (8), using $M = 100$ data points.

graphically verifies Eq. (6) and the developed numerical discretization of Eq. (6) [6].

Figure 8 presents temperature data with white noise at $r = r_1$ and $r = r_2$ using the previously described input parameter set, however, with $\omega_m = 0.025$, $m = 1$, 2. The solid circles represent the noisy temperature data generated in accordance to Eq. (9), the dashed lines represent the filtered data in accordance to Eq. (7), and the solid lines represent the numerical results from the analytic temperature solutions. It is difficult to discern any difference between the filtered (dashed) and exact (solid) temperatures at $r = r_1$ and $r = r_2$.

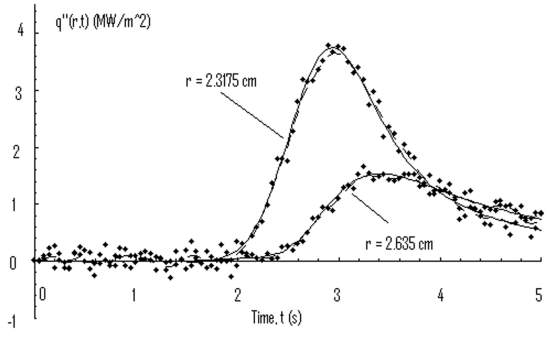

Fig. 9 Heat flux results using noisy temperature data displayed in Fig. 8 at $r = r_1 = 2.3175$ cm, $r = r_2 = 2.635$ cm over time, t: exact (solid line), discrete noisy [solid circles, based on Eq. (1)], and filtered [dashed lines, based on Eq. (1)] for material having $\alpha = 0.1$ cm^2/s, $k = 50$ W/(m°C), and imposed Gauss heat flux boundary condition, Eq. (8), using $M = 100$ data points.

Figure 9 presents the resulting heat fluxes at the probe sites using both the filtered (dashed line) and unfiltered (solid circles) data sets as predicted based on Eq. (1) or Eq. (6). Again, the solid lines represent numerical results based on the exact solution. There exists a reduction in oscillatory magnitude about the exact heat flux (solid line) after the temperature data have gone through the digital low-pass filter. Here, $n_c = 13$ and is estimated based on the power spectra of the temperature signal, in accordance with signal-to-noise reasoning [6]. Hence, a substantial reduction in the root-mean-square heat flux error results.

Conclusions

The newly derived early-time integral relationship between temperature and heat flux leads to a transient means for determining the local heat flux $q''(r, t)$ for $r \geq a$ in a hollow cylinder having infinite outer radius. More important, this new relationship explicitly exhibits the need to estimate or represent the heating rate accurately for estimating the heat flux. This geometry has practical implications for several aerospace studies. The local heat flux is obtained from either filtered temperature data [6] or directly from a heating/cooling rate sensor [8]. The latter can lead to nearly real-time predictions of the heat flux. Digital filtering can be placed into a running form for real-time applications. The applicability of the asymptotic solution depends on the sensor radial location, thermal diffusivity, and time. Equation (1) demonstrates that the local inverse problem for recovering the heat flux from the time history of temperature is possible and actually can be determined from a temperature sensor.

Appendix: Derivation of the Early-Time Temperature–Heat Flux Integral Relationship

Consider the geometry displayed in Figs. 2 and 3, where it is our intent to develop a relationship between heat flux and heating rate to illustrate the importance of the heating rate for accurately estimating the heat flux based on the time history of the temperature. Following conventional Green's function doctrine (or a boundary element method), the temperature $T(r, t)$, $r \geq \eta$, $t \geq 0$ can be expressed as

$$w_r T(r,t) = -\eta\alpha \int_{t_0=0}^{t} \left[G(r, t/\eta, t_0) \frac{\partial T}{\partial r_0}(\eta, t_0) - T(\eta, t_0) \frac{\partial G}{\partial r_0}(r, t/\eta, t_0) \right] \mathrm{d}t_0, \qquad r \geq \eta, \qquad t \geq 0 \quad \text{(A1a)}$$

or, recalling the definition of heat flux as obtained from Fourier's law, we obtain

$$w_r T(r,t) = \eta\alpha \int_{t_0=0}^{t} \left[G(r, t/\eta, t_0) \frac{q''(\eta, t_0)}{k} + T(\eta, t_0) \frac{\partial G}{\partial r_0}(r, t/\eta, t_0) \right] \mathrm{d}t_0, \qquad r \geq \eta, \qquad t \geq 0 \quad \text{(A1b)}$$

where the Green's function $G(r, t/r_o, t_o)$ is given in Eq. (4d). The weight function conforms with the boundary element method and is set to unity for $r > \eta$. Using Fourier's law, we can obtain the corresponding heat flux, $q''(r, t)$ as

$$w_r q''(r,t) = -k \frac{\partial T}{\partial r}(r,t) = -k\eta\alpha \int_{t_o=0}^{t} \left[\frac{\partial G}{\partial r}(r, t/\eta, t_o) \frac{q''(\eta, t_o)}{k} + T(\eta, t_o) \frac{\partial^2 G}{\partial r \partial r_o}(r, t/\eta, t_o) \right] \mathrm{d}t_o, \qquad r \geq \eta, \qquad t \geq 0 \quad \text{(A2)}$$

Next, we replace the Green's function $G(r, t/r_0, t_0)$ with $\tilde{G}(r, t/r_0, t_0)$ under the assumption that $rr_0/[2\alpha(t - t_0)] \to \infty$ or, since $r > \eta$, this implies small times. Recasting Eqs. (A1b) and (A2) to reflect the asymptotic study, we have

$$\tilde{T}(r,t)=\eta\alpha\int_{t_0=0}^{t}\left[\tilde{G}(r,t/\eta,t_0)\frac{\tilde{q}''(\eta,t_0)}{k}+\tilde{T}(\eta,t_0)\frac{\partial\tilde{G}}{\partial r_0}(r,t/\eta,t_0)\right]\mathrm{d}t_0,\qquad r>\eta,\qquad z\to\infty \quad \text{(A3)}$$

and

$$\tilde{q}''(r,t)=-k\eta\alpha\int_{t_0=0}^{t}\left[\frac{\partial\tilde{G}}{\partial r}(r,t/\eta,t_0)\frac{\tilde{q}''(\eta,t_0)}{k}+\tilde{T}(\eta,t_0)\frac{\partial^2\tilde{G}}{\partial r\partial r_0}(r,t/\eta,t_0)\right]\mathrm{d}t_0,\qquad r>\eta,\qquad z\to\infty \quad \text{(A4)}$$

where we consider $r>\eta$ (hence $w_r=1$), and we denote the corresponding early-time temperature and heat flux as $\tilde{T}(r,t)$ and $\tilde{q}''(r,t)$, respectively, and where the Green's function $\tilde{G}(r,t/r_0,t_0)$ is given in Eq. (5c). Frankel et al. [1–7] have developed a rigorous mathematical approach for developing the desired integral relationship in planar geometries.

To begin the derivation, we express Eqs. (A3) and (A4) in explicit terms as

$$\tilde{T}(r,t)=\frac{\sqrt{\eta\alpha}}{4\pi\sqrt{r\pi}}\int_{t_0=0}^{t}\left[\frac{\tilde{q}''(\eta,t_0)}{k}\frac{e^{-\frac{(r-\eta)^2}{4\alpha(t-t_0)}}}{\sqrt{t-t_0}}+\tilde{T}(\eta,t_0)\frac{e^{-\frac{(r-\eta)^2}{4\alpha(t-t_0)}}}{2\sqrt{t-t_0}}\times\left(-\frac{1}{\eta}+\frac{r-\eta}{\alpha(t-t_0)}\right)\right]\mathrm{d}t_o,\qquad r>\eta,\qquad z\to\infty \quad \text{(A5)}$$

and

$$\tilde{q}''(r,t)=-\frac{k\sqrt{\eta\alpha}}{8\pi\sqrt{r\pi}}\int_{t_0=0}^{t}\left[-\frac{\tilde{q}''(\eta,t_0)}{k}\frac{e^{-\frac{(r-\eta)^2}{4\alpha(t-t_0)}}}{\sqrt{t-t_0}}\left(\frac{1}{r}+\frac{r-\eta}{\alpha(t-t_0)}\right)+\frac{\tilde{T}(\eta,t_0)}{2}\frac{e^{-\frac{(r-\eta)^2}{4\alpha(t-t_0)}}}{\sqrt{t-t_0}}\left(\frac{1}{r\eta}-\frac{(r-\eta)^2}{[\alpha(t-t_0)]^2}+\frac{(r-\eta)^2}{\alpha r\eta(t-t_0)}+\frac{2}{\alpha(t-t_0)}\right)\right]\mathrm{d}t_0,\qquad r>\eta,\qquad z\to\infty \quad \text{(A6)}$$

To obtain an integral relationship between temperature and heat flux at an arbitrary location, we need to eliminate the integrals involving the boundary conditions at $r=\eta$. Frankel [6] has proposed a regularization approach based on the nature of the kernels involved. To this end, we let $t\to s$ in Eq. (A5), and then operate on this with

$$\int_{s=0}^{t}\frac{\mathrm{d}s}{\sqrt{t-s}}$$

to get

$$\int_{s=0}^{t}\frac{\tilde{T}(r,s)}{\sqrt{t-s}}\,\mathrm{d}s=\frac{\sqrt{\eta\alpha}}{4\pi\sqrt{r\pi}}\int_{s=0}^{t}\frac{1}{\sqrt{t-s}}\times\int_{t_0=0}^{s}\left[\frac{\tilde{q}''(\eta,t_0)}{k}\frac{e^{-\frac{(r-\eta)^2}{4\alpha(s-t_0)}}}{\sqrt{s-t_0}}+\tilde{T}(\eta,t_0)\frac{e^{-\frac{(r-\eta)^2}{4\alpha(s-t_0)}}}{2\sqrt{s-t_0}}\times\left(-\frac{1}{\eta}+\frac{r-\eta}{\alpha(s-t_0)}\right)\right]\mathrm{d}t_0\mathrm{d}s,\qquad r>\eta,\qquad z\to\infty \quad \text{(A7)}$$

Next, we integrate the left-hand side by parts and carefully interchange the order of integration on the right-hand side to obtain

$$2\int_{s=0}^{t}\frac{\partial\tilde{T}}{\partial s}(r,s)\sqrt{t-s}\,\mathrm{d}s=\frac{\sqrt{\eta\alpha}}{4\pi\sqrt{r\pi}}\int_{t_0=0}^{t}\left[\frac{\tilde{q}''(\eta,t_0)}{k}\int_{s=t_0}^{t}\frac{e^{-\frac{(r-\eta)^2}{4\alpha(s-t_0)}}}{\sqrt{s-t_0}\sqrt{t-s}}\,\mathrm{d}s+\frac{\tilde{T}(\eta,t_0)}{2}\left(-\frac{1}{\eta}\int_{s=t_0}^{t}\frac{e^{-\frac{(r-\eta)^2}{4\alpha(s-t_0)}}}{\sqrt{s-t_0}\sqrt{t-s}}\,\mathrm{d}s+\frac{r-\eta}{\alpha}\times\int_{s=t_0}^{t}\frac{e^{-\frac{(r-\eta)^2}{4\alpha(s-t_0)}}}{(s-t_0)^{\frac{3}{2}}\sqrt{t-s}}\,\mathrm{d}s\right)\right]\mathrm{d}t_0,\qquad r>\eta,\qquad z\to\infty \quad \text{(A8)}$$

where we noted that the initial condition was $T(r,0)=0^\circ\mathrm{C}$ and [6]

$$\int_{s=t_0}^{t}\frac{e^{-\frac{(r-\eta)^2}{4\alpha(s-t_0)}}}{\sqrt{s-t_0}\sqrt{t-s}}\,\mathrm{d}s=\pi erfc\sqrt{\frac{(r-\eta)^2}{4\alpha(t-t_0)}} \quad \text{(A9a)}$$

and

$$\int_{s=t_0}^{t}\frac{e^{-\frac{(r-\eta)^2}{4\alpha(s-t_0)}}}{(s-t_0)^{\frac{3}{2}}\sqrt{t-s}}\,\mathrm{d}s=\sqrt{4\pi\alpha}\frac{e^{-\frac{(r-\eta)^2}{4\alpha(t-t_0)}}}{\sqrt{(r-\eta)^2}\sqrt{t-t_0}} \quad \text{(A9b)}$$

where $(r-\eta)^2/(4\alpha)>0$ and $erfc(v)$ represents the complementary error function with argument v. Substituting Eqs. (A9a) and (A9b) into Eq. (A8) produces

$$2\int_{t_0=0}^{t}\frac{\partial\tilde{T}}{\partial t_0}(r,t_0)\sqrt{t-t_0}\,\mathrm{d}t_0=\sqrt{\frac{\eta\alpha}{16\pi r}}\int_{t_0=0}^{t}\left[\frac{\tilde{q}''(\eta,t_0)}{k}erfc\sqrt{\frac{(r-\eta)^2}{4\alpha(t-t_0)}}+\frac{\tilde{T}(\eta,t_0)}{2}\left(-\frac{1}{\eta}erfc\sqrt{\frac{(r-\eta)^2}{4\alpha(t-t_0)}}+\frac{2}{\sqrt{\pi\alpha}}\frac{e^{-\frac{(r-\eta)^2}{4\alpha(t-t_0)}}}{\sqrt{t-t_0}}\right)\right]\mathrm{d}t_0,\qquad r>\eta,\qquad z\to\infty \quad \text{(A10)}$$

where we also replaced the dummy variable s by t_0 on the left-hand side for mere cosmetics. Next, we differentiate Eq. (A10) with respect to time t to get

$$\int_{t_0=0}^{t}\frac{\partial\tilde{T}}{\partial t_0}(r,t_0)\frac{\mathrm{d}t_0}{\sqrt{t-t_0}}=\frac{r-\eta}{8\pi k}\sqrt{\frac{\eta}{r}}\int_{t_0=0}^{t}\tilde{q}''(\eta,t_0)\frac{e^{-\frac{(r-\eta)^2}{4\alpha(t-t_0)}}}{(t-t_0)^{\frac{3}{2}}}\,\mathrm{d}t_0+\frac{1}{8\pi}\sqrt{\frac{\eta}{r}}\int_{t_0=0}^{t}\tilde{T}(\eta,t_0)\frac{e^{-\frac{(r-\eta)^2}{4\alpha(t-t_0)}}}{(t-t_0)^{\frac{3}{2}}}\left(-\frac{r-\eta}{2\eta}+\frac{(r-\eta)^2}{2\alpha(t-t_0)}-1\right)\mathrm{d}t_0,\qquad r>\eta,\qquad z\to\infty \quad \text{(A11)}$$

Next, let us return to Eq. (A6) and multiply it by $\sqrt{\alpha\pi}/k$, then regroup terms to get

$$\frac{\sqrt{\alpha\pi}}{k}\tilde{q}''(r,t) = \frac{\alpha}{8\pi k r}\sqrt{\frac{\eta}{r}}\int_{t_0=0}^{t}\tilde{q}''(\eta,t_0)\frac{e^{-\frac{(r-\eta)^2}{4\alpha(t-t_0)}}}{\sqrt{t-t_0}}\,\mathrm{d}t_0 + \frac{r-\eta}{8\pi k}\sqrt{\frac{\eta}{r}}\int_{t_0=0}^{t}\tilde{q}''(\eta,t_0)\frac{e^{-\frac{(r-\eta)^2}{4\alpha(t-t_0)}}}{(t-t_0)^{\frac{3}{2}}}\,\mathrm{d}t_0 - \frac{\alpha}{16\pi}\sqrt{\frac{\eta}{r}}\int_{t_0=0}^{t}\tilde{T}(\eta,t_0)\frac{e^{-\frac{(r-\eta)^2}{4\alpha(t-t_0)}}}{\sqrt{t-t_0}}\left(\frac{1}{r\eta}-\frac{(r-\eta)^2}{[\alpha(t-t_0)]^2} + \frac{(r-\eta)^2}{\alpha r\eta(t-t_0)}+\frac{2}{\alpha(t-t_0)}\right)\Bigg]\mathrm{d}t_0, \qquad r>\eta, \qquad z\to\infty \tag{A12}$$

Let us now return to Eq. (A5) and multiply it by $\sqrt{\alpha\pi}/(2r)$ to get

$$\frac{\sqrt{\alpha\pi}}{2r}\tilde{T}(r,t) = \frac{\alpha}{8\pi k r}\sqrt{\frac{\eta}{r}}\int_{t_0=0}^{t}\tilde{q}''(\eta,t_0)\frac{e^{-\frac{(r-\eta)^2}{4\alpha(t-t_0)}}}{\sqrt{t-t_0}}\,\mathrm{d}t_0 + \frac{\alpha}{16\pi r}\sqrt{\frac{\eta}{r}}\int_{t_0=0}^{t}\tilde{T}(\eta,t_0)\frac{e^{-\frac{(r-\eta)^2}{4\alpha(t-t_0)}}}{\sqrt{t-t_0}}\left(-\frac{1}{\eta} + \frac{r-\eta}{\alpha(t-t_0)}\right)\mathrm{d}t_0, \qquad r>\eta, \qquad z\to\infty \tag{A13}$$

Observe that the two integrals on the right-hand side of Eq. (A11) can be eliminated with the aid of Eqs. (A12) and (A13). Upon making these substitutions and performing the algebraic manipulation, we arrive at the significant relationship

$$\tilde{q}''(r,t) = \frac{k\tilde{T}(r,t)}{2r} + \sqrt{\frac{\rho Ck}{\pi}}\int_{t_0=0}^{t}\frac{\partial\tilde{T}}{\partial t_0}(r,t_0)\frac{\mathrm{d}t_0}{\sqrt{t-t_0}}, \qquad r>\eta, \qquad t\geq 0 \tag{A14}$$

This expression is similar to the half-space planar relationship, but now contains the extra geometric term $k\tilde{T}(r,t)/(2r)$. Equation (A14) is valid for $r^2/(2\alpha t)\gg 1$ and we have, for simplicity, removed the asymptotic notation.

References

[1] Frankel, J. I., Osborne, G. E., and Taira, K., "Stabilization of Ill-Posed Problems Through Thermal Rate Sensors," *Journal of Thermophysics and Heat Transfer*, Vol. 20, No. 2, 2006, pp. 238–246. doi:10.2514/1.9136

[2] Frankel, J. I., and Lawless, J. J., "Numerically Stabilizing Ill-Posed Moving Surface Problems Through Heat Rate Sensors," *Journal of Thermophysics and Heat Transfer*, Vol. 19, No. 4, 2005, pp. 587–592. doi:10.2514/1.11057

[3] Frankel, J. I., and Arimilli, R. V., "Inferring Convective and Radiative Heating Loads from Transient Surface Temperature Measurements in the Half-Space," *Inverse Problems in Sciences and Engineering*, Vol. 15, No. 5, 2007, pp. 463–488.

[4] Frankel, J. I., Keyhani, M., Arimilli, R. V., and Wu, J., "A New Multidimensional Integral Relationship Between Heat Flux and Temperature for Direct Internal Assessment of Heat Flux," *Zeitschrift fur Angewandte Mathematik und Physik (ZAMP)* [online journal], Aug. 2007. doi:10.1007/s00033-007-6135-6

[5] Frankel, J. I., "Generalizing the Method of Kulish to One-Dimensional Unsteady Heat Conducting Slabs," *Journal of Thermophysics and Heat Transfer*, Vol. 20, No. 4, 2006, pp. 945–950. doi:10.2514/1.22995

[6] Frankel, J. I., "Regularization of Inverse Heat Conduction by Combination of Rate Sensors Analysis and Analytic Continuation," *Journal of Engineering Mathematics*, Vol. 57, No. 2, 2007, pp. 181–198. doi:10.1007/s10665-006-9073-y

[7] Frankel, J. I., and Kulish, V. V., "A New Flux Integral Relationship for Half-Space Transient Heat Conduction with Arbitrary Initial Condition," *Engineering Analysis with Boundary Elements*, Vol. 32, No. 2, 2008, pp. 162–167. doi:10.1016/j.enganabound.2007.07.008

[8] Frankel, J. I., Arimilli, R. V., Keyhani, M., and Wu, J., "Heating Rate $\mathrm{d}T/\mathrm{d}t$ Measurements Developed from In-Situ Thermocouples Using a Voltage-Rate Interface for Advanced Thermal Diagnostics," *25th AIAA Aerodynamics Measurement Technology and Ground Testing Conference*, AIAA Paper No. 2006-3636, 2006.

[9] Kulish, V. V., Lage, J. L., Komarov, P. L., and Raad, P. E., "A Fractional-Diffusion Theory for Calculating Thermal Properties of Thin Films from Surface Transient Thermoreflectance Measurements," *Journal of Heat Transfer*, Vol. 123, No. 6, 2001, pp. 1133–1138. doi:10.1115/1.1416688

[10] Kulish, V. V., and Lage, J. L., "Fractional Diffusion Solutions for Transient Local Temperature and Heat Flux," *Journal of Heat Transfer*, Vol. 122, No. 2, 2000, pp. 372–376. doi:10.1115/1.521474

[11] Kress, R., *Linear Integral Equations*, Springer–Verlag, Berlin, 1989.

[12] Wing, G. M., *A Primer on Integral Equations of the First Kind*, SIAM, Philadelphia, PA, 1991.

[13] Linz, P., *Analytical and Numerical Methods for Volterra Equations*, Society for Industrial and Applied Mathematics, Philadelphia, 1985.

[14] Ozisik, M. N., *Heat Conduction*, Wiley, New York, 1980, Chap. 3.

[15] Brebbia, C. A., Telles, J. C. F., and Wrobel, L. C., *Boundary Element Techniques*, Springer–Verlag, New York, 1984.

[16] Frankel, J. I., Vick, B., and Ozisik, M. N., "Flux Formulation in Hyperbolic Heat Conduction," *Journal of Applied Physics*, Vol. 58, No. 9, 1985, pp. 3340–3345. doi:10.1063/1.335795

[17] Butkovskiy, A. G., *Green's Functions and Transfer Functions Handbook*, Ellis Horwood, London, 1984, pp. 54–68.

[18] Beck, J. V., Cole, K. D., Haji-Sheikh, A., and Litkouhi, B., *Heat Conduction Using Green's Functions*, Hemisphere, New York, 1992, pp. 441–443.

[19] Buttsworth, D. R., and Jones, T. V., "Radial Conduction Effects in Transient Heat Transfer Experiments," *The Aeronautical Journal*, Vol. 101, 1997, pp. 209–212.